Faraday Discussions

Accepted Manuscript

This manuscript will be presented and discussed at a forthcoming Faraday Discussion meeting. All delegates can contribute to the discussion which will be included in the final volume.

Register now to attend! Full details of all upcoming meetings: http://rsc.li/fd-upcoming-meetings

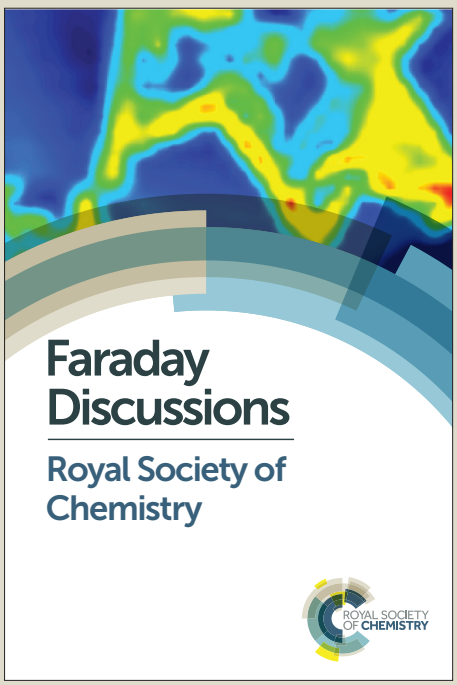

This is an *Accepted Manuscript*, which has been through the Royal Society of Chemistry peer review process and has been accepted for publication.

Accepted Manuscripts are published online shortly after acceptance, before technical editing, formatting and proof reading. Using this free service, authors can make their results available to the community, in citable form, before we publish the edited article. We will replace this *Accepted Manuscript* with the edited and formatted *Advance Article* as soon as it is available.

You can find more information about *Accepted Manuscripts* in the Information for Authors.

Please note that technical editing may introduce minor changes to the text and/or graphics, which may alter content. The journal's standard Terms & Conditions and the Ethical guidelines still apply. In no event shall the Royal Society of Chemistry be held responsible for any errors or omissions in this *Accepted Manuscript* or any consequences arising from the use of any information it contains.

ROYAL SOCIETY OF CHEMISTRY

www.rsc.org/faraday_d

New *In-Situ* Solid-State NMR Techniques for Probing the Evolution of Crystallization Processes: Pre-Nucleation, Nucleation and Growth

*Colan E. Hughes, P. Andrew Williams, Victoria L. Keast, Vasileios G. Charalampopoulos, Gregory R. Edwards-Gau and Kenneth D. M. Harris**

School of Chemistry, Cardiff University, Park Place, Cardiff CF10 3AT, Wales, U.K.

** Author for Correspondence (E-mail: HarrisKDM@cardiff.ac.uk)*

Abstract

The application of *in-situ* techniques for investigating crystallization processes promises to yield significant new insights into fundamental aspects of crystallization science. With this motivation, we recently developed a new *in-situ* solid-state NMR technique that exploits the ability of NMR to selectively detect the solid phase in heterogeneous solid/liquid systems (of the type that exist during crystallization from solution), with the liquid phase "invisible" to the measurement. As a consequence, the technique allows the first solid particles produced during crystallization to be observed and identified, and allows the evolution of different solid phases (e.g., polymorphs) present during the crystallization process to be monitored as a function of time. This *in-situ* solid-state NMR strategy has been demonstrated to be a powerful approach for establishing the sequence of solid phases produced during crystallization and for the discovery of new polymorphs. The most recent advance of the *in-situ* NMR methodology has been the development of a strategy (named "CLASSIC NMR") that allows *both* solid-state NMR *and* liquid-state NMR spectra to be measured (essentially simultaneously) during the crystallization process, yielding information on the complementary changes that occur in both the solid and liquid phases as a function of time. In this article, we present new results that highlight the application of our *in-situ* NMR techniques to successfully unravel different aspects of crystallization processes, focusing on: (i) the application of a CLASSIC NMR approach to monitor competitive inclusion processes in solid urea inclusion compounds, (ii) exploiting liquid-state NMR to gain insights into co-crystal formation between benzoic acid and pentafluorobenzoic acid, and (iii) applications of *in-situ* solid-state NMR for the discovery of new solid forms of trimethylphosphine oxide and L-phenylalanine. Finally, the article

discusses a number of important fundamental issues relating to practical aspects, the interpretation of results and the future scope of these techniques, including: (i) an assessment of the smallest size of solid particle that can be detected in *in-situ* solid-state NMR studies of crystallization, (ii) an appraisal of whether the rapid sample spinning required by the NMR measurement technique may actually influence or perturb the crystallization behaviour, and (iii) a discussion of factors that influence the sensitivity and time-resolution of *in-situ* solid-state NMR experiments.

1. Introduction

Crystal nucleation and growth processes [1, 2] are encountered in many different scientific fields and are crucially important in many aspects of chemical, pharmaceutical and biological sciences. Progress to improve our fundamental understanding of crystallization processes has important practical applications, including the development of new ways to exert control over the polymorphic form of crystals produced in industrial applications. Deepening our fundamental physico-chemical understanding of crystallization relies significantly on the development and application of new experimental strategies, particularly those that allow direct *in-situ* monitoring of the process. In general, crystallization processes are governed by kinetic factors and meta-stable polymorphs are often produced rather than the thermodynamically stable polymorph (in this context, polymorphs [3-10] are defined as crystalline materials that have identical chemical composition but different crystal structures). Furthermore, crystallization processes often evolve through a sequence of different solid forms before reaching the final crystallization product and details of the time-evolution of the process can depend critically on the exact conditions of the crystallization experiment. In order to optimize and control crystallization in such situations, it is essential to understand the sequence of events involved in the evolution of the solid form, rather than simply characterizing the final crystalline phase collected at the end of the process. In this regard, experimental strategies that allow direct *in-situ* monitoring of crystallization processes are clearly essential. A wide variety of experimental techniques have been used for *in-situ* studies of crystallization [11], including scattering techniques (e.g., X-ray diffraction, small-angle X-ray scattering, neutron diffraction and small-angle neutron scattering), spectroscopic methods (e.g., infrared, Raman or X-ray absorption spectroscopies) and microscopy (e.g., atomic force microscopy). However, until the present time, solid-state NMR spectroscopy has not been used extensively in this regard.

Although solid-state NMR is a powerful and versatile technique for investigating structural and dynamic properties of solids, adapting this technique for *in-situ* studies of chemical processes is associated with specific technical challenges. These challenges include the fact that high-resolution solid-state NMR spectra are usually recorded under conditions of rapid sample spinning (at frequencies typically around 10,000 revolutions per second) and the fact that the system under

investigation must be located in a sealed rotor within a confined and relatively inaccessible space inside the magnet of the solid-state NMR spectrometer. For these reasons, the development of *in-situ* solid-state NMR techniques has typically lagged behind other *in-situ* experimental methods.

Recently, we developed a new *in-situ* solid-state NMR technique [12, 13] for monitoring the evolution of the solid phase as a function of time during crystallization from solution. This technique has been shown to yield new insights into several issues relating to crystallization processes, particularly the time-evolution of different polymorphs (or other solid forms) and the transformations between polymorphs that occur during the crystallization process. Very recently [14], we proposed and demonstrated an extension of the *in-situ* NMR strategy involving *combined* liquid-state and solid-state NMR measurements. This new implementation of the strategy, termed "CLASSIC NMR" (**C**ombined **L**iquid- **A**nd **S**olid-**S**tate ***I**n-situ* **C**rystallization NMR), allows the evolution of *both* the solid phase *and* the liquid phase to be probed as a function of time during the same crystallization experiment, yielding significantly deeper insights on the behaviour of the entire crystallization system.

After giving an overview of the foundations of these *in-situ* solid-state NMR techniques, including illustrative examples of their applications, we focus on presenting new results that highlight the capability of *in-situ* solid-state NMR to deepen our understanding of crystallization processes. In addition, a critical discussion of several fundamental aspects of the methodology is presented. Issues covered include an appraisal of the possible effects of rapid sample rotation (an intrinsic requirement for recording high-resolution solid-state NMR data) and sample confinement on the pathways and outcome of crystallization processes, and an assessment of the extent to which knowledge gained from *in-situ* NMR studies may be exploited in the optimization of bulk crystallization experiments.

2. Essential Background to High-Resolution Solid-State NMR

A basic premise underlying the development of solid-state NMR for *in-situ* studies of crystallization processes is the well-established fact that high-resolution solid-state NMR can be utilized for identification of different polymorphic forms of solids [5, 9, 15]. In the case of organic solids, for example, the high-resolution solid-state ^{13}C NMR spectrum contains, in principle, one peak for each

crystallographically distinguishable carbon atom in the crystal structure (although, in practice, the actual number of *observed* peaks may be less than this number as a consequence of accidental peak overlap). The peak positions (i.e., the isotropic chemical shifts) in the high-resolution solid-state ^{13}C NMR spectrum depend both on the environment of the ^{13}C nucleus within the molecule and also on the local environment surrounding the ^{13}C nucleus within the crystal structure. As a consequence, for a given ^{13}C site within an organic molecule, the peak positions in high-resolution solid-state ^{13}C NMR spectra can typically differ within a range of about ±5 ppm between different polymorphs (or other solid forms) due to the dependence of the isotropic chemical shift on the crystal structure. Of course, larger differences in peak positions may arise between polymorphs that contain significantly different conformations or different tautomeric forms of the molecule. In this section, we give a very brief introduction to the experimental methods for measuring high-resolution solid-state NMR spectra of powder samples of organic solids.

In the case of high-resolution solid-state ^{13}C NMR of organic solids with natural isotopic abundances, the primary contributions to line-broadening arise from chemical shift anisotropy and from direct ^{13}C–^{1}H dipole-dipole interactions. The line-broadening is reduced (resulting in high-resolution ^{13}C NMR spectra) by a combination of rapid magic-angle sample spinning (MAS) [16], typically at spinning frequencies of around 10 kHz, and high-power ^{1}H decoupling.

Another experimental technique that is commonly applied in the measurement of high-resolution solid-state ^{13}C NMR spectra of organic materials is $^{1}H \rightarrow {}^{13}C$ cross polarization (CP) [9, 17-19]. In this technique, rather than directly exciting the ^{13}C nuclei followed by detection of the ^{13}C NMR signal, the procedure is to excite the ^{1}H nuclei, followed by transfer of magnetization from the ^{1}H nuclei to the ^{13}C nuclei (i.e., the "cross-polarization" process) and detection of the resulting ^{13}C NMR signal. In the measurement of high-resolution solid-state ^{13}C NMR spectra of powder samples, the major benefit of using $^{1}H \rightarrow {}^{13}C$ CP is that it gives a significant enhancement of signal intensity compared to normal direct-excitation ^{13}C NMR measurements.

In the context of applying high-resolution solid-state ^{13}C NMR for *in-situ* studies of crystallization from solution, the use of $^{1}H \rightarrow {}^{13}C$ CP has the critical additional benefit of allowing selective detection of the ^{13}C NMR signal *only* from the solid component of the heterogeneous

solid/liquid system that exists during the crystallization process (see Section 3 for more details). An important aspect of the $^{1}H \rightarrow ^{13}C$ CP technique is that the recycle delay in the NMR experiment (the time between successive applications of the pulse sequence) is dictated by ^{1}H spin-lattice relaxation (and not by ^{13}C spin-lattice relaxation). This feature is advantageous because, for organic materials, ^{1}H spin-lattice relaxation times (T_1) are typically much shorter than ^{13}C spin-lattice relaxation times, allowing more rapid repetition of the pulse sequence (in general, the recycle delay is taken as $5 \times T_1$), hence reducing the time required to record the solid-state ^{13}C NMR spectrum. For direct excitation ^{13}C NMR measurements, on the other hand, the recycle delay is dictated by the ^{13}C spin-lattice relaxation and, therefore, typically requires longer recycle delays than for $^{1}H \rightarrow ^{13}C$ CP measurements.

More details of these techniques and other technical aspects of solid-state NMR can be found elsewhere [18, 19].

3. Experimental Aspects of *In-Situ* Solid-State NMR Studies of Crystallization Processes

In our *in-situ* solid-state NMR strategy for monitoring crystallization processes, a homogeneous (undersaturated) solution is initially prepared inside the NMR rotor at elevated temperature (T_H) and crystallization is then induced by decreasing the temperature rapidly to a specific target temperature (T_L) at which the solution is supersaturated (Fig. 1). Crystallization is thermodynamically favoured at the target temperature and the time-dependence of the crystallization process is monitored by repeatedly recording high-resolution solid-state NMR spectra as a function of time.

Clearly, the time-resolution of the *in-situ* monitoring of the crystallization process depends on the time required to record an individual NMR spectrum of adequate quality to identify and distinguish the different solid forms present during the evolution of the system. Thus, optimization of the sensitivity of the measurement is also important, allowing solid-state NMR spectra of adequate quality to be recorded in the shortest possible time. More discussion of sensitivity and time-resolution in *in-situ* NMR studies of crystallization is given in Section 6.4.

As discussed in Section 2, sufficiently good spectral resolution is also required in order to identify and assign the solid phases present at different stages of the crystallization process. Clearly,

it is desirable to be able to detect and identify the first solid particles produced in the crystallization process, although at this stage the amount of solid present in the crystallization system is generally very low. Maximizing the sensitivity of the NMR measurement is thus also very important for enhancing the prospects for observing very early stages of the process.

Prior to our development of the *in-situ* NMR techniques described above, the prospect of using solid-state NMR for *in-situ* studies of crystallization from solution was limited by the difficulty of securely sealing a fluid phase inside an NMR rotor such that MAS could be carried out at several kHz without problems arising from leakage of the liquid from the rotor. Fortunately, advances in rotor technology (see Fig. 12 in Section 6) that allow solutions to be securely sealed inside NMR rotors for MAS experiments have taken place in recent years and this technical development paved the way for the types of experiment described here.

An important feature of the *in-situ* solid-state NMR strategy is that it exploits the opportunity afforded by NMR of complete selectivity in detecting <u>*only*</u> the solid component in the crystallization system, such that the dissolved solute and solvent are undetected in the measurement. In the case of organic materials, such discrimination between solid and solution phases is achieved by recording ^{13}C NMR spectra under conditions of $^{1}H \rightarrow ^{13}C$ cross polarization (CP). As molecules in the solid phase and the solution phase generally have substantially different dynamic behaviour, measurements under normal conditions for $^{1}H \rightarrow ^{13}C$ CP give rise to a signal <u>*only*</u> from the solid phase. Thus, even if only a small fraction of the solute has crystallized (e.g., in the early stages of crystallization), only the solid particles contribute to the measured NMR spectrum, while the dissolved solute molecules (present in much greater amount in the early stages of crystallization) are "invisible" to the measurement.

In contrast, for *in-situ* studies of crystallization processes based on X-ray or neutron scattering techniques, scattering occurs *both* from the crystalline solid particles (giving rise to Bragg diffraction peaks) *and* from the solution phase (giving rise to a broad background scattering). As a result, the scattering data may be dominated by the contribution from the solution phase, particularly in the early stages of the crystallization process when the amount of the solid phase is low. Furthermore, it is important to emphasize that, in the *in-situ* solid-state NMR experiment,

essentially the entire crystallization system (i.e., the sample inside the NMR rotor) is studied. In the case of *in-situ* X-ray or neutron scattering experiments, on the other hand, a finely focused incident beam is used, which typically interrogates only a fraction of the sample inside the *in-situ* cell. Finally, we note that, unlike the situation for diffraction-based techniques, solid-state NMR has no requirement that the sample must be crystalline. Thus, high-resolution solid-state NMR spectra can be measured both for crystalline and amorphous solids, and therefore *in-situ* solid-state NMR studies of crystallization processes provide the opportunity to observe both crystalline and amorphous solid forms that may be produced at different stages of the process.

4. Illustrative Examples of Applications of *In-Situ* Solid-State NMR Techniques to Study Crystallization Processes

4.1 Monitoring Polymorphic Evolution During Crystallization

Glycine ($H_3^+NCH_2CO_2^-$) is widely adopted as a model system for studies of crystallization and polymorphism [20-38]. Under ambient conditions, three polymorphs of glycine (denoted α, β and γ) are known [20-24], with relative stabilities γ > α > β [28, 39]. The three polymorphs are readily distinguished by high-resolution solid-state ^{13}C NMR as the isotropic ^{13}C chemical shift for the carboxylate group is distinctly different in the three polymorphs (176.5, 175.5 and 174.5 ppm for the α, β and γ polymorphs respectively) [30]. The consensus in the literature is that crystallization from water at neutral pH produces the meta-stable α polymorph. However, an early publication suggested [22] that crystallization from deuterated water may promote the formation of the γ polymorph, although systematic studies of this isotope effect were reported only recently [34, 36], in which it was demonstrated *inter alia* that deuteration (even at levels as low as 1%) does significantly increase the probability of obtaining the γ polymorph. Crystallization of glycine from methanol/water is reported [32] to promote the formation of the β polymorph.

To explore the effect of deuteration, we carried out separate *in-situ* solid-state ^{13}C NMR studies [12] of crystallization of glycine from water with natural isotopic abundances (H_2O; Fig. 2a) and from deuterated water (D_2O; Fig. 2b) (in the latter case, the total level of deuteration of all exchangeable hydrogen sites in the system was 86%). In crystallization from H_2O, we simply observe the formation and growth of the α polymorph as a function of time, with no other

polymorphs observed throughout the duration (13 hr) of the experiment. In crystallization from D_2O, the α polymorph is again observed as the first solid form, suggesting that the same nucleation pathway is followed in both H_2O and D_2O. However, about 1.5 hr after commencing the experiment, a peak characteristic of the γ polymorph appears in the ^{13}C NMR spectrum. The amount of the γ polymorph then increases rapidly while the amount of the α polymorph diminishes at the same rate, consistent with a solution-mediated polymorphic transformation. For each of the two isotopomeric systems, the final polymorph obtained at the end of the *in-situ* solid-state NMR study is consistent with the preferred polymorphic outcome in conventional laboratory crystallization experiments carried out under the same conditions and over the same total period of time.

To investigate the growth and stability of the β polymorph, crystallization was initiated by adding methanol to an aqueous solution of glycine [32] in an NMR rotor just prior to insertion into the NMR spectrometer for the *in-situ* solid-state ^{13}C NMR study (Fig. 2c) [13]. In the first spectrum recorded, the solid is identified as a virtually pure sample of the β polymorph (with a very small amount of the α polymorph also present). The amount of the β polymorph then decreases progressively, transforming into the α polymorph. Clearly, the *in-situ* solid-state ^{13}C NMR study allows the timescale of this polymorphic transformation to be established and indicates that a viable strategy for isolating the β polymorph would be to stop the crystallization experiment within a few minutes of triggering the crystallization process.

Another example of polymorphic evolution has been revealed by *in-situ* solid-state ^{13}C NMR studies of crystallization of *m*-aminobenzoic acid (*m*-ABA) from methanol. Five polymorphs of *m*-ABA are known [40, 41] and the crystal structures of four polymorphs (Forms II, III, IV and V) have been determined. In Forms I, III and IV, the *m*-ABA molecules exist as zwitterions whereas, in Forms II and V, the *m*-ABA molecules are non-zwitterionic. Each polymorph is uniquely distinguished by its high-resolution solid-state ^{13}C NMR spectrum [14]. In laboratory crystallization experiments, the outcome of crystallization of *m*-ABA from methanol is unpredictable, yielding either Form I, Form III or mixtures of Forms I and III. Our *in-situ* solid-state ^{13}C NMR study led to a full understanding of this situation, as the results demonstrate clearly that Form I is the initial crystallization product, followed by a polymorphic transformation (within a few hours of the formation of Form I) to produce Form III. Thus, depending on the time at which crystals are

collected in laboratory crystallization experiments, the product may be either pure Form I, a mixture of Forms I and III, or pure Form III.

4.2 Discovery of New (Unknown) Solid Forms by In-Situ Solid-State NMR Studies

The examples discussed so far highlight the capability of the *in-situ* solid-state NMR strategy to observe transient polymorphs on the pathway to the final crystallization product, in cases for which these polymorphs were already *known* and well characterized. Clearly, *in-situ* solid-state NMR studies also have the potential to reveal new (previously unknown) polymorphs that may exist during crystallization processes [42]. In such cases, the results provide unique insights on the specific crystallization conditions required to produce each new polymorph observed, including the appropriate "time-window" during which a specific new polymorph is present.

To illustrate the discovery of new solid forms, we consider an *in-situ* solid-state ^{13}C NMR study of co-crystal formation involving urea and 1,10-dihydroxydecane. Co-crystals of even-chain α,ω-dihydroxyalkanes [$HO(CH_2)_nOH$ with n = 6, 8, 10, 12, 14, 16] and urea (in 1:2 molar ratio) have been shown [43] to exhibit well-defined structure types characterized by two features: (i) double-stranded hydrogen-bonded urea ribbons in which the two strands are either *parallel* or *antiparallel*, and (ii) an angle between the axis of the α,ω-dihydroxyalkane and the positive direction of the urea strand which is either *acute* or *obtuse*. Specifically, the *antiparallel/acute* structure is found for n = 6, the *parallel/acute* structure is found for n = 8 and the *antiparallel/obtuse* structure is found for n = 10 – 16. Surprisingly, in laboratory crystallization experiments using a wide range of different conditions, no polymorphism has been observed for any member of this family. However, in the *in-situ* solid-state ^{13}C NMR study of the crystallization of 1,10-dihydroxydecane and ^{13}C-labelled urea from methanol, the ^{13}C chemical shift for the initial crystallization product is clearly different from that of the known co-crystal phase (Fig. 3). After about 40 min, a new peak characteristic of the known co-crystal phase appears and thereafter grows very rapidly. At the end of the experiment (11.4 hr), only the known co-crystal phase is present (confirmed by *ex-situ* powder X-ray diffraction). Comparison of the ^{13}C chemical shift for urea in the new solid form present in the early stages of the crystallization process with those for urea in other members of the family of α,ω-dihydroxyalkane-$(urea)_2$ co-crystals leads to the assignment that

the new transient solid form is a 1,10-dihydroxydecane-(urea)$_2$ co-crystal with the *parallel/acute* structure type.

4.3 CLASSIC NMR

As discussed in Section 3, the *in-situ* solid-state NMR methodology has recently been extended to exploit the fact that a solid-state NMR spectrometer can be used to study *both* the liquid phase *and* the solid phase in a heterogeneous solid/liquid system, simply by changing the pulse sequence used to record the NMR data. Specifically, by alternating between two different pulse sequences in an *in-situ* NMR study of crystallization, alternate solid-state NMR and liquid-state NMR spectra are recorded, yielding essentially simultaneous information on the time-evolution of *both* the solid phase *and* the liquid phase during the crystallization process (Fig. 4). This strategy (called "CLASSIC NMR") reveals the complementary changes that occur in the solid phase and in the liquid phase as a function of time during crystallization. The time-dependence of the amount and polymorphic identity of the solid phase is established from the solid-state NMR spectra, while changes in the solution-state speciation and modes of molecular aggregation in solution are monitored from the time-evolution of the liquid-state NMR spectrum. Although critical nucleation entities are generally too small to be observed (see Section 6.1), understanding the conditions under which nucleation takes place potentially allows improved models for nucleation to be proposed.

The CLASSIC NMR strategy has been demonstrated [14] in a ^{13}C NMR study of crystallization of *m*-aminobenzoic acid (*m*-ABA) from dimethyl sulfoxide (DMSO). Selective detection of the solid phase was achieved using ^{1}H→^{13}C CP with high-power ^{1}H decoupling, while selective detection of the liquid phase was achieved using direct ^{13}C excitation with no ^{1}H decoupling and a relatively short recycle delay (the absence of ^{1}H decoupling and the short recycle delay ensure that no significant signal is detected from the solid phase).

The solid-state component of the CLASSIC ^{13}C NMR data showed that, about 2 hr after the start of the measurements, Form I of *m*-ABA appeared, with the amount then increasing during the next 6 hr. No other polymorphs were observed during the crystallization process. The liquid-state component of the CLASSIC ^{13}C NMR data also did not change for the first 2 hr of the experiment (i.e., the period before crystallization commenced), after which significant changes were observed.

The integrated intensity of the peaks for *m*-ABA in the liquid-state NMR spectra decreased during the next 6 hr, reflecting the fact that the solution phase becomes progressively more dilute as crystallization proceeds.

Significantly, systematic changes are observed in the liquid-state ^{13}C chemical shifts for *m*-ABA and the solvent DMSO as a function of time during the crystallization process (some peaks shift to more positive chemical shifts and other peaks shift to more negative chemical shifts). At the start of the measurement, the system is a supersaturated solution. After crystallization begins, the supersaturation decreases with time and by the end of the crystallization process, the system is an equilibrium saturated solution. It is known from independent studies that, in an equilibrium saturated solution of *m*-ABA in DMSO, the *m*-ABA molecules exist in the non-zwitterionic form. From this knowledge, and by rationalizing the change in the ^{13}C chemical shift for each ^{13}C site in *m*-ABA observed as a function of time during the CLASSIC NMR experiment, significant insights can be gained on the nature of the supersaturated solution that exists at the start of the crystallization experiment. Specifically, the observed changes in liquid-state ^{13}C chemical shifts are consistent with the supersaturated solution of *m*-ABA in DMSO at the start of the crystallization experiment having **(a)** a higher proportion of zwitterionic *m*-ABA molecules and/or **(b)** a higher proportion of non-zwitterionic *m*-ABA molecules present in hydrogen-bonded aggregates, relative to a saturated solution of *m*-ABA in DMSO. Both scenarios **(a)** and **(b)** represent an increased degree of protonation of the NH_2 group of *m*-ABA and are plausible solution-state precursors to the $O^{-}\cdots H–N^{+}$ hydrogen bonds that exist between *m*-ABA zwitterions in the crystal structure of Form I. Although we cannot distinguish whether situation **(a)** or situation **(b)** is predominant, the CLASSIC NMR results nevertheless give clear insights into the nature of the speciation and interactions that exist in the supersaturated pre-nucleation solution of *m*-ABA in DMSO prior to crystallization, relative to those in the saturated solution at the end of the crystallization process.

5. New Results From *In-Situ* NMR Studies of Crystallization Processes

5.1 Monitoring Competitive Inclusion Processes in Solid Inclusion Compounds by a CLASSIC NMR Approach

Recently, we have exploited the opportunity to use *in-situ* NMR to explore the crystallization of conventional urea inclusion compounds with a variety of long chain alkane and α,ω-dibromoalkane guest molecules. In these solid inclusion compounds [44-49], "guest" molecules are densely packed along one-dimensional tunnels in a hexagonal, hydrogen-bonded urea "host" structure (Fig. 5). In particular, we have investigated the competition between alkane and α,ω-dibromoalkane guest molecules for inclusion into the urea host tunnel structure during crystal growth. In these competitive crystallization experiments, two types of potential guest molecule are present in the solution phase and compete for inclusion within the urea host structure.

We report a combined liquid-state and solid-state *in-situ* NMR study of crystallization from a solution comprising urea, 1,8-dibromooctane and tetradecane (approximate molar ratios 10:1:2, respectively) in methanol. The solution was prepared at 50 °C and then cooled to 20 °C at a constant rate over 11 hr. Direct-excitation ^{13}C NMR spectra were recorded (with ^{1}H decoupling) throughout the cooling process and for a further 6 hr after reaching 20 °C. In contrast to most organic solids, the guest molecules in urea inclusion compounds undergo rapid reorientational motions within the urea host tunnel structure. As a consequence, direct-excitation ^{13}C NMR spectra recorded under conditions normally used to record liquid-state ^{13}C NMR spectra detect a signal from the guest molecules in the solid urea inclusion compounds. Thus, the direct-excitation ^{13}C NMR spectra recorded in the *in-situ* study of crystallization of urea inclusion compounds contain signals from the guest molecules *both* in the solid urea inclusion compounds *and* in the liquid phases present. On the other hand, $^{1}H \rightarrow ^{13}C$ CP measurements give much weaker signals for the guest molecules in the urea inclusion compounds. Consequently, only direct-excitation ^{13}C NMR spectra were recorded in the present case (Fig. 6).

The peak assignments in the *in-situ* ^{13}C NMR spectra (see Fig. 6) are made by reference to samples of urea inclusion compounds and solutions prepared independently of the *in-situ* ^{13}C NMR study. At the start of the *in-situ* study (at 50 °C), both 1,8-dibromooctane and tetradecane are

present (together with urea) dissolved in methanol and peaks are observed in the ^{13}C NMR due to these components. However, an additional set of peaks is present, arising from a separate liquid phase of pure tetradecane (clearly, under the conditions of this experiment, the tetradecane was only partially dissolved in the methanol solution). As the system is cooled, the amount of the liquid phase of tetradecane diminishes and new peaks emerge concomitantly in positions characteristic of tetradecane guest molecules in the urea host structure. Significantly, no peaks are present in the positions expected for 1,8-dibromooctane guest molecules in the urea host structure, clearly indicating the preferential inclusion of tetradecane over 1,8-dibromooctane in the formation of the urea inclusion compound. Indeed, it is well established [50] that inclusion of longer guest molecules over shorter guest molecules is favoured within a homologous family, although the nature of end-group substituents on the guest molecules may also influence the preferential uptake of guest molecules within the urea tunnel structure.

Fig. 7 shows the relative amounts of tetradecane in the three different phases as a function of time during the crystallization process (determined by integration of the peak for the methyl group in each phase). The amount of tetradecane in the solution phase remains essentially constant throughout the experiment, whereas the amount of the pure liquid tetradecane phase decreases and the amount of tetradecane guest molecules in the solid urea inclusion compound increases. From these results, it is clear that the formation of the urea inclusion compound containing tetradecane guest molecules occurs within the solution phase. Moreover, while tetradecane is consumed from the solution phase by this process, it is clear from Fig. 7 that the partitioning of tetradecane between the solution phase and the pure liquid tetradecane phase adjusts in order to maintain a constant concentration within the solution phase, leading to a diminution in the amount of the pure liquid tetradecane phase present as a function of time.

5.2 Exploiting Liquid-State NMR to Gain Insights on Crystallization Processes

In some cases, long $T_1(^1H)$ relaxation times for organic solids are such that the recycle delays required to record solid-state ^{13}C NMR spectra using the $^1H \rightarrow ^{13}C$ CP technique are very long. In such cases, the time to record an individual solid-state ^{13}C NMR spectrum within the context of an *in-situ* NMR study of crystallization would be prohibitively long to allow acceptable time-

resolution in monitoring the process. In such cases, however, liquid-state ^{13}C NMR spectra can still be recorded quickly (as ^{13}C spin-lattice relaxation times for the liquid phase are significantly shorter) and may still yield significant insights into the processes occurring. This situation is encountered for benzoic acid and its derivatives.

Following an initial *in-situ* liquid-state ^{13}C NMR study of crystallization of benzoic acid [51], we report here studies of crystallization from a solution containing equimolar amounts of benzoic acid (BA) and pentafluorobenzoic acid (PFBA) in d_2-dichloromethane. BA and PFBA are known to form a 1:1 co-crystal [52] in which the two components exist exclusively as hetero-molecular BA···PFBA pairs, linked by the well-known double hydrogen-bonded carboxylic acid dimer motif. A relevant question is whether all possible solution-state pairings BA···BA, BA···PFBA and PFBA···PFBA exist in the solution state prior to crystallization and whether there is any change in the nature of these interactions as crystallization proceeds.

Ex-situ studies indicate that the known co-crystal phase is the only crystallization product from this solvent. However, very distinct behaviour is observed in our *in-situ* liquid-state NMR studies of the crystallization process. Fig. 8 shows the results from separate *in-situ* ^{1}H NMR and *in-situ* ^{19}F NMR studies of crystallization from a solution comprising BA and PFBA (in 1:1 molar ratio) in d_2-dichloromethane (with time resolution of 28 s for the ^{1}H NMR study and 25 s for the ^{19}F NMR study) [53]. In both sets of data, a sudden change in chemical shifts is observed (at 38 min in the ^{1}H NMR data and at 10 min in the ^{19}F NMR data), corresponding to very fast co-crystal formation. The existence of a lag time before crystallization occurs and variability in the length of this lag time in different experiments is typical for this system and explains the difference in the time at which the sudden change in chemical shifts occurs in the *in-situ* ^{1}H NMR and ^{19}F NMR experiments.

In the *in-situ* ^{1}H NMR spectra, the largest change in ^{1}H chemical shift occurs for the carboxylic acid group, which shifts by *ca*. –0.4 ppm. The fact that only one ^{1}H resonance is observed for the carboxylic acid groups in the system indicates that rapid proton exchange must occur between BA and PFBA molecules, as well as between different interaction environments of these molecules (e.g., the BA···BA, BA···PFBA and PFBA···PFBA hydrogen-bonded pairings).

The ^{1}H chemical shifts for the phenyl ring of BA move in the opposite direction by *ca*. +0.1 ppm. The change in the ^{1}H chemical shift for the carboxylic acid groups suggests that, in the supersaturated solution that exists prior to crystallization, the proportion of molecules in solution that exist in hydrogen-bonded dimers is higher than that in the more dilute solution that exists at the end of the crystallization process (it is well established that the ^{1}H chemical shift of carboxylic acids is more positive for a hydrogen-bonded dimer than a non-hydrogen bonded monomer). In the *in-situ* liquid-state ^{19}F NMR study, the three ^{19}F chemical shifts all move in the same direction by between +0.06 ppm and +0.23 ppm. This observation suggests that the aryl rings of both the BA and PFBA molecules in the solution state experience similar changes as a consequence of the rapid decrease in solution-state concentration that accompanies crystallization, probably indicative of a change in the extent of π-stacking of the aromatic rings of both BA and PFBA molecules.

Overall, there is no evidence to suggest that BA and PFBA molecules are segregated in the solution phase (e.g., if the solution phase comprised only BA···BA and PFBA···PFBA pairs, then clearly two ^{1}H signals would be observed for carboxylic acid groups). However, while a proportion of hydrogen-bonded BA···PFBA pairs must exist to account for the presence of only one carboxylic acid peak in the ^{1}H NMR spectra, we cannot rule out the presence of BA···BA and PFBA···PFBA pairs in rapid proton exchange with the BA···PFBA pairs.

5.3 Polymorph Discovery

An example illustrating the discovery of a hitherto unknown solid phase concerns our *in-situ* solid-state ^{31}P NMR study of crystallization of trimethylphosphine oxide (TMPO) from toluene. Only one crystal structure has been reported for TMPO, with one molecule in the asymmetric unit (and hence one ^{31}P NMR environment). Correspondingly, the solid-state ^{31}P NMR spectrum of a powder sample of TMPO has only one isotropic peak and a single peak in each spinning sideband. In the *in-situ* ^{31}P NMR study of crystallization from toluene, even the first spectrum recorded (see Fig. 9) reveals that a substantial amount of solid was present at the earliest stages of the crystallization process. Interestingly, this spectrum has two isotropic peaks, while each spinning sideband is a single peak. One isotropic peak corresponds to the known phase of TMPO, while the new isotropic peak (indicated in Fig. 9) must represent a new solid form of TMPO. The observation that the ^{31}P

NMR spectrum of the new solid form has an isotropic peak with no spinning sidebands under the $^{1}H \rightarrow ^{31}P$ CPMAS NMR measurement conditions is intriguing and suggests that the TMPO molecules are in a dynamic regime that is sufficiently slow to allow a signal to be generated in $^{1}H \rightarrow ^{31}P$ CP but sufficiently rapid to average the ^{31}P chemical shift anisotropy such that spinning sidebands are eliminated. We propose that the additional isotropic peak observed in the crystallization of TMPO may arise from an amorphous phase or perhaps a rotator phase solid (we note that the shape of the TMPO molecule is almost isotropic, given the similar steric character of the oxygen and methyl substituents, which is a common feature in rotator phase materials).

5.4 A New Solid Form of L-Phenylalanine

Recently, L-phenylalanine (L-Phe) has been shown to display abundant polymorphism, with four polymorphs reported so far. The first form to be structurally characterized [54], now denoted form I of L-Phe, has recently been re-determined [55] (including correction of an earlier reported "re-determination" [56]). In the past two years, three new polymorphs have been reported, one discovered by our group, denoted form II [57], followed by form III [58] and form IV [55]. Our work [57] also revealed the existence of monohydrate and hemihydrate phases of L-Phe.

In-situ solid-state ^{13}C NMR studies have been carried out on the crystallization of L-Phe from ethanol/water. Under these conditions, L-Phe has been reported [59] to produce a solid form different to the only polymorph (form I) that was known at that time. The results of our *in-situ* ^{13}C NMR study are shown in Fig. 10, together with solid-state ^{13}C NMR spectra recorded for powder samples of the monohydrate and hemihydrate of L-Phe and form I of anhydrous L-Phe. Although the *in-situ* ^{13}C NMR data were recorded at high magnetic field (20 T corresponding to a ^{13}C Larmor frequency of 213.8 MHz) over 21 hr, the signal-to-noise ratio is rather low as a result of slow ^{1}H spin-lattice relaxation (requiring a long recycle delay in the NMR measurement) and a low concentration of the crystallization solution (resulting in only a small amount of the solid phase being formed). In spite of the poor quality of the *in-situ* ^{13}C NMR data, however, new peaks (particularly around 147 ppm; see Fig. 10) are clearly identified that are not present in the ^{13}C NMR spectra of other solid forms of L-Phe shown in Fig. 10, specifically form I of L-Phe and the hemihydrate and monohydrate phases (solid-state ^{13}C NMR spectra of the other polymorphs of

L-Phe have not been measured as form II can only be prepared by rigorous drying of the hemihydrate and we have not attempted to prepare forms III and IV). However, periodic DFT calculations using the CASTEP code (Accelrys, San Diego, CA) [60] (which allows NMR spectra to be calculated from known crystal structures [61, 62]) indicate that the ^{13}C NMR spectra of forms II and III do not have an isotropic peak with ^{13}C chemical shift around 147 ppm. DFT could not be applied to form IV as the crystal structure is disordered.

At this stage, the new solid form observed in the *in-situ* solid-state NMR study is not yet identified, although the three primary possibilities are: (i) form IV, (ii) a new polymorph of L-Phe, or (iii) a new solvate of L-Phe. A new solvate phase is perhaps the most likely, although no ethanol solvates of L-Phe have been reported. Nevertheless, we note that the hemihydrate and monohydrate phases are channel hydrates with closely related structures (in which the water molecules are located in channels created by the packing of L-Phe molecules), with form II of anhydrous L-Phe essentially representing the "empty" channel structure [57]. It is certainly plausible to suggest that other types of solvent molecules, such as ethanol, could be accommodated within this L-Phe channel structure. Attempts to isolate the new solid form (to allow crystal structure determination and other analysis) have so far been unsuccessful.

6. A Critical Appraisal of Practical Aspects, Interpretation of Results and the Scope and Limitations of *In-situ* NMR Studies of Crystallization Processes

In this section, we discuss a number of issues that are relevant to the practical implementation of the *in-situ* solid-state NMR methodology, as well as considering important factors that serve to define the scope and limitations of the technique. In this discussion, we address some key questions that are often raised about the *in-situ* solid-state NMR technique, including: (i) what is the smallest size of solid particle that can be detected, and (ii) is the crystallization process influenced by the application of the rapid sample rotation required to record high-resolution solid-state NMR spectra?

6.1 *What is the Smallest Size of Solid Particle that can be Detected in In-situ Solid-State NMR Studies of Crystallization?*

A question frequently asked in connection with our technique relates to the smallest size of solid particle that can be observed in the *in-situ* cross-polarization (CP) NMR measurements, with implications on the earliest stage of the crystallization process that can actually be detected. Unfortunately, establishing this limit experimentally is very challenging. One experimental approach could be to carry out systematic studies of a set of samples each consisting of solid particles with a known, narrow range of sizes in liquid suspension. However, we have not been able to obtain a suitable set of samples of this nature. Consequently, we estimate the limiting size based on theoretical considerations.

As emphasized above, a key feature of our *in-situ* solid-state NMR strategy is that selectivity in measuring only the NMR spectrum of the solid phase may be achieved by the use of a CP pulse sequence. The key limitation for obtaining a signal by CP is the rate of tumbling of the solid particle, since this motion "scrambles" the orientation of the dipolar couplings responsible for the polarization transfer. The tumbling motion is characterized by a correlation time, τ_c, which is related to the volume (V) of the particle, the viscosity (η) of the solvent and temperature (T), through the Stokes-Einstein-Debye relation [63]

$$\tau_c = \frac{6V\eta}{k_B T\, l(l+1)}, \qquad [1]$$

where l is the order of the spherical harmonic for the interaction ($l = 2$ for dipolar coupling). Nowacka *et al.* [64] established that, for a $^{1}H \rightarrow ^{13}C$ CP experiment to give a signal under similar conditions to those used in our experiments, the limiting value of τ_c is *ca.* 10 μs. Using Eq. 1 and taking the bulk viscosity of water (~10^{-3} Pa s), the limiting volume is estimated to be $V \approx 4 \times 10^{7}$ Å^3, corresponding to a sphere with radius of around 210 Å. To put this value in context, particles of glycine of this size would contain around 5×10^{5} molecules. Although a number of approximations and assumptions are inherent in this derivation, it nevertheless offers a reasonable estimate of the smallest size of solid particle that could be detected in an *in-situ* solid-state NMR study of crystallization. Clearly, the estimate could be refined in any particular case by taking into

account known features of the experimental conditions, such as knowledge of the viscosity of the solution.

Although the size of the critical nucleation entity in crystallization from solution may vary significantly between different crystallization systems and for a given crystallization system under different experimental conditions, it is anticipated that the critical clusters involved in the nucleation of most organic materials would comprise significantly fewer than 5×10^5 molecules. Thus, the smallest solid particles that are observable under the conditions of *in-situ* solid-state NMR studies are likely to represent post-nucleation stages of the crystallization process. Nevertheless, as illustrated in the case of crystallization of glycine from methanol/water in Section 4.1, identification of the polymorphic form of the earliest solid particles detected in the crystallization process can nevertheless provide important clues about the probable nucleation pathway, which cannot be obtained from *ex-situ* identification of the final crystallization product collected at the end of the crystallization process.

6.2 Does the NMR Measurement Technique Itself Influence the Crystallization Process?

Another important question is whether the rapid sample rotation required to record high-resolution solid-state NMR spectra may actually affect the pathway and/or the final outcome of the crystallization process. More broadly, it is important to consider the effects of all the physical conditions that the crystallization system is subjected to in our experiments, including (i) the pressure exerted on the sample due to rapid spinning, (ii) the nature of the rotor materials in contact with the sample and (iii) the containment of the sample under the mother liquor throughout the experiment.

With regard to (i), the pressure distribution within a sample subjected to spinning in a cylindrical rotor can be calculated if the density distribution is known. Specifically, the pressure imposed by sample spinning is given by

$$p(r) = \omega^2 \int_{r_0}^{r} \rho(r') r' dr', \qquad [2]$$

where ω is the spinning frequency in rad s^{-1} and $\rho(r)$ is the density of the sample at distance r from the rotation axis of the rotor (see Fig. 11). The term r_0 represents the radius of any cylindrical void present at the centre of the rotor (and co-axial with the rotation axis), which arises if the sample does not completely fill the rotor. If the density is assumed to be constant throughout the sample, Eq. 2 simplifies to

$$p(r) = \tfrac{1}{2}\omega^2(r^2 - r_0^2)\rho\,. \qquad [3]$$

Although the assumption of uniform density may be justifiable in some cases (e.g., for samples with low compressibility), a more realistic form of Eq. 3 would take into account the distribution of density of the sample inside the rotor (i.e., $\rho(r)$ as in Eq. 1). In the case of a homogeneous solution inside the rotor prior to crystallization, the solution must respond to the pressure gradient (lowest pressure at the centre of the rotor and greatest pressure at the walls) by redistribution of mass towards the outer part of the rotor to create a density gradient across the sample (again, with lowest density at the centre of the rotor and greatest density at the walls). Such a density gradient may have important implications for the ensuing crystallization process, as it may result in a non-uniform distribution of concentration across the solution. Furthermore, given the distribution of pressure within the spinning sample (and the fact that solubility is a function of pressure), the solubility may also be non-uniform across the sample. Clearly, the confluence of these issues creates significantly more complex crystallization conditions than those that exist in a conventional laboratory crystallization experiment, and a more detailed quantitative understanding of the effects of sample rotation is merited. Intuitively, however, we anticipate that the inhomogeneities introduced into the crystallization system as a consequence the sample spinning probably represent relatively minor non-uniformities which, in the majority of cases, will not significantly affect the behaviour of the crystallization process.

Returning to the question of pressure, we note that the pressure at the walls of the rotor is independent of the density distribution through the sample and is given by

$$p(r_i) = \tfrac{1}{2}\omega^2(r_i^2 - r_0^2)\rho_{av}, \qquad [4]$$

where r_i is the internal radius of the rotor and ρ_{av} is the average density of the sample, equal to the static density in the absence of compression. Under these circumstances, Eq. 4 becomes

$$p(r_i) = \frac{m\omega^2}{2\pi L} \quad [5]$$

where m is the total mass of the sample and L is the length of the sample cavity in the rotor.

Using Eq. 4, for a rotor with internal radius $r_i = 1.5$ mm containing water and spinning at MAS frequency $\omega = 12$ kHz with a cylindrical void $r_0 = 0.5$ mm at the centre of the rotor, the pressure at the rotor walls is $p(r_i) = 57$ atm. This value rises to $p(r_i) = 64$ atm for a full rotor (i.e., $r_0 = 0$) at the same MAS frequency. Armed with these values, it is possible to assess the effect of spinning on the crystals formed in the *in-situ* NMR experiment in comparison to high pressure studies on powder samples. In the case of glycine, for example, the pressures observed to induce polymorphic transformations (≥ 0.5 GPa or 5000 atm) [65-69] are significantly higher than those generated in the NMR rotor subjected to MAS. Nevertheless, polymorphism in other systems could be affected by pressures of the order of those generated by MAS, as observed previously in *in-situ* solid-state NMR studies of dehydration of sodium acetate trihydrate [70]. In this case, the dehydration process was found to lead to a different distribution of the polymorphs of anhydrous sodium acetate when the dehydration was carried out under conditions of rapid sample spinning compared to dehydration of a static (non-spinning) sample.

Sample rotors for MAS NMR experiments are composed of a sleeve and one or two sealing caps (depending on whether the sleeve is open at one end or both ends). Schematics of two different designs of sealing system are shown in Fig. 12. The sleeves are usually made from zirconia, whilst the caps may be composed of a variety of materials including Kel-F® and Teflon® with some designs using silicone or fluorosilicone rubber O-rings. Clearly, these materials interact with the crystallization solution and may potentially play a role in the nucleation process [33].

Finally, another key distinction between *in-situ* NMR experiments and *ex-situ* studies of crystallization is that the *in-situ* NMR technique observes the crystallization product directly within the crystallization solution without removal from the mother liquor. Potentially, this feature could lead to differences in the solid form observed in the *in-situ* NMR study compared to the form observed in laboratory crystallization experiments in which the crystallization product is characterized *ex situ* (e.g., by powder X-ray diffraction or solid-state NMR) following removal from

the crystallization solution. Clearly, it is well known that certain solid forms may only be stable when submerged in the mother liquor and transform rapidly to a more stable form on removal from the crystallization solution.

It is clear from the issues discussed in this section that certain aspects of the instrumentation and experimental methodology required to carry out *in-situ* solid-state NMR studies of crystallization from solution have the potential to influence the pathway and outcome of the crystallization process, including (perhaps most importantly) the effect of the pressure generated in the solution by rapid sample spinning and the consequent effect on the density distribution within the solution. However, in our experience so far, we have not yet observed any systems for which the *final* solid form(s) extracted from the NMR rotor following an *in-situ* crystallization study does not match the *final* solid form(s) resulting from crystallization in the laboratory under the same conditions and carried out over a comparable period of time.

6.3 Some Practical Aspects

An important practical aspect of our *in-situ* NMR studies of crystallization processes is accurate temperature calibration. This issue is particularly crucial with regard to ensuring reliable transferability of experimental information derived from normal laboratory experiments (e.g., information on solubilities of materials and crystallization conditions required to produce specific polymorphs, etc.) into the context of *in-situ* NMR studies. In our experience, the temperature control equipment on NMR spectrometers is often inaccurate for samples undergoing MAS, largely due to the heating effect of the rapid sample spinning but also due to a lack of adequate calibration of the equipment. Consequently, we rely on calibrated values of temperature which incorporate the heating effect of MAS at the specific MAS frequency used. The discrepancy between the temperature indicated by the temperature control equipment and the actual temperature can be as large as 30 °C. We use calibrations based on measurements on lead nitrate [71] and methanol [72-74]. A calibration using glycol is also available for higher temperatures than those covered by the methanol calibration [72].

As discussed in Section 3, a technical advance that was pivotal to the successful development of the *in-situ* solid-state NMR technique was the availability of NMR rotors that can be used for

magic-angle spinning of liquid containing samples, without leakage of liquid. Depending upon the type of NMR rotor used, various sealing systems are available (see Fig. 12). An important practical consideration for these rotors is whether the solvent to be used in a crystallization experiment is compatible with the material used to manufacture the seals on the rotor. While water is compatible with all such materials, certain organic solvents may soften the rotor materials, leading to leakage of liquid particularly at the elevated temperature required to achieve dissolution.

6.4 Sensitivity and Time-Resolution

As mentioned in Section 3, achieving sufficiently good time resolution in *in-situ* solid-state NMR studies is an essential requirement for observing all the phases involved in the crystallization process, including short-lived solid forms that have only transient existence. Clearly, the time-resolution of the *in-situ* study is dictated by the time required to record an individual NMR spectrum with adequate signal-to-noise ratio to allow the solid forms present to be identified. A number of factors are important in this regard, including: (i) the NMR receptivity of the selected nucleus, (ii) the applied magnetic field strength, (iii) the NMR relaxation properties and (iv) the total amount of solid phase that can be produced in the crystallization experiment.

First, the NMR receptivity of a selected nucleus depends on fundamental properties of the nucleus and on the natural isotopic abundance. The only opportunity for the experimenter to increase the receptivity is to increase the isotopic abundance by using an isotopically labelled sample. Of the nuclei discussed here, the natural isotopic abundances are ^{1}H (99.99%), ^{13}C (1.05%), ^{19}F (100%) and ^{31}P (100%), so the prospect of isotopic labelling is relevant only in the case of ^{13}C NMR. Clearly, ^{13}C labelling is highly desirable for *in-situ* ^{13}C NMR studies, although it is not always essential and may not be feasible for synthetic reasons. However, to illustrate the advantages of ^{13}C labelling, the *in-situ* solid-state ^{13}C NMR study of crystallization of 1,10-dihydroxydecane/urea (using ^{13}C-labelled urea) discussed in Section 4.2 had a time-resolution of 2.7 min [42] whereas the solid-state component of the CLASSIC ^{13}C NMR study of crystallization of *m*-ABA from DMSO (using natural isotopic abundances) discussed in Section 4.3 had a time-resolution of 38.4 min [14].

Second, in order to achieve maximum sensitivity in NMR measurements and hence to achieve the best possible time-resolution for *in-situ* studies, the experiments should be carried out using an NMR spectrometer with the highest available applied magnetic field. For this reason, most of our recent research on the application of the techniques described here has been carried out at the UK National High-Field (850 MHz) Solid-State NMR Facility.

Third, as discussed in Section 2, the main sample-dependent factor controlling the time required to record an NMR spectrum is the recycle delay (the time delay that must be left between successive applications of the NMR pulse sequence) which depends on the spin-lattice relaxation time (T_1) of one type of nucleus present in the material. In the case of solid-state ^{13}C NMR spectra recorded using ^{1}H→^{13}C CP, the recycle delay is dictated by the ^{1}H spin-lattice relaxation time [75]. In the case of organic solids, the presence of a mobile group (e.g., methyl or ammonium) in the molecule usually ensures that $T_1(^1\text{H})$ is less than 1 s (for molecules of the size we have typically investigated). However, in the absence of a mobile group, $T_1(^1\text{H})$ is generally much longer. Clearly, solid-state ^{13}C NMR spectra can be recorded much more rapidly for materials with short $T_1(^1\text{H})$, which is conducive for good time-resolution in *in-situ* solid-state ^{13}C NMR studies of crystallization of organic materials.

Finally, the total amount of the solid phase that can be produced in the crystallization experiment clearly depends on the concentration of the solute and the differential of solubility as a function of temperature, recalling that, in our *in-situ* NMR strategy, crystallization is induced by decrease of temperature. Thus, in our experimental protocol, the solute must be completely soluble at the high temperature (T_H) at which the homogeneous solution is prepared and should be insoluble at low temperature (T_L) at which the *in-situ* NMR measurements are carried out. Thus, if the molality of the initial solution prepared at T_H is denoted m_o, and using s to denote solubility, we require that $S(T_H) > m_o$ and $S(T_L) < m_o$. Clearly, at some temperature (T_C) between T_H and T_L, the system must satisfy $S(T_C) = m_o$ and crystallization becomes thermodynamically favoured for $T \leq T_C$. Clearly, to ensure that a significant amount of solid phase is produced during the crystallization experiment, the difference in solubilities $S(T_C) - S(T_L)$ should be as large as possible. Hence, for a given crystallization system, the three factors under the control of the experimenter (i.e., the molality m_o and temperature T_H at the start of the experiment and the target crystallization

temperature T_L) should be chosen such that T_H is as high as possible, T_L is as low as possible and m_o should be only slightly lower than $S(T_H)$. Under these circumstances, T_C lies close to T_H and the difference in solubilities $S(T_C) - S(T_L)$ is maximized (for a given value of T_L).

For a given magnetic field strength, we have found that the "worst case scenario" occurs when the absolute change in solubility, $S(T_C) - S(T_L)$, is small, the isotopic abundance of the observed nucleus is low, and $T_1(^1H)$ is long (e.g., longer than 30 s). Under such conditions, even at high applied magnetic field, acquisition of a solid-state NMR signal on a timescale useful for studying crystallization processes is probably impossible. However, if just one of the three factors is favourable, we can reasonably expect to be able to observe the crystallization process with adequate time-resolution, especially when measurements are carried out at high applied magnetic field.

7. Concluding Remarks

We have shown, both in our previous publications [12-14, 42, 51] and in the new results discussed in this paper, that *in-situ* solid-state NMR studies offer a variety of new opportunities for studying different aspects of crystallization processes. These opportunities include observing polymorphic evolution, discovering new polymorphs and other solid phases, developing strategies for preparing unstable polymorphs and identifying changes in the solution state that occur during the crystallization process. In each case, *in-situ* NMR yields information that cannot be obtained from *ex-situ* studies or, in some cases, from other *in-situ* experimental techniques. In particular, the recently developed CLASSIC NMR experiment extends significantly the scope and capability of *in-situ* monitoring of crystallization processes as it is unique in providing simultaneous and complementary information on the time-evolution of *both* the liquid *and* solid phases during crystallization. We forecast with confidence that further developments of the methodology for *in-situ* NMR studies of crystallization, together with the application of these techniques to a wide range of different types of systems, will significantly advance our fundamental understanding of crystallization processes in the years to come.

Acknowledgments

We are grateful to EPSRC (studentship funding to VKL and GREG) and Agilent (studentship funding to VKL) for financial support, and to the Action «Supporting Postdoctoral Researchers» of the Operational Program "Education and Lifelong Learning" (Action's Beneficiary: General Secretariat for Research and Technology of Greece), co-financed by the European Social Fund and the Greek State, for a postdoctoral fellowship to VGC (Project Code: PE4 1236). We are grateful to the UK 850 MHz Solid-State NMR Facility for the award of significant amounts of time for *in-situ* solid-state NMR studies of crystallization. This facility is funded by EPSRC, BBSRC and the University of Warwick, including part funding through Birmingham Science City Advanced Materials Projects 1 and 2 supported by Advantage West Midlands and the European Regional Development Fund. We particularly appreciate the assistance of the Facility Manager, Dr Dinu Iuga.

References

1. B. Kahr and J. M. McBride, *Angew. Chem. Int. Ed.* **31**, 1-26 (1992).
2. *Crystal Growth and Nucleation, Faraday Discussions*, Vol. 136, 2007, RSC Publishing.
3. J. D. Dunitz, *Pure Appl. Chem.* **63**, 177-185 (1991).
4. J. Bernstein, *Polymorphism in Molecular Crystals*, IUCr Monographs on Crystallography, 2002, Oxford University Press, Oxford.
5. R. J. Davey, *Chem. Comm.* 1463-1467 (2003).
6. J. Bernstein, *Chem. Comm.* 5007-5012 (2005).
7. S. Chen, H. Xi and L. Yu, *J. Am. Chem. Soc.* **127**, 17439-17444 (2005).
8. S. Ahn, F. Guo, B. M. Kariuki and K. D. M. Harris, *J. Am. Chem. Soc.* **128**, 8441-8452 (2006).
9. R. K. Harris, *Analyst* **131**, 351-373 (2006).
10. S. L. Price, *Acc. Chem. Res.* **42**, 117-126 (2008).
11. N. Pienack and W. Bensch, *Angew. Chem. Int. Ed.* **50**, 2014-2034 (2011).

12. C. E. Hughes and K. D. M. Harris, *J. Phys. Chem. A* **112**, 6808-6810 (2008).

13. C. E. Hughes and K. D. M. Harris, *Chem. Comm.* **46**, 4982-4984 (2010).

14. C. E. Hughes, P. A. Williams and K. D. M. Harris, *Angew. Chem. Int. Ed.* **53**, 8939-8943 (2014).

15. K. D. M. Harris and J. M. Thomas, *J. Solid State Chem.* **94**, 197-205 (1991).

16. E. R. Andrew, A. Bradbury and R. G. Eades, *Nature* **1958**, 1802-1803 (1959).

17. S. R. Hartmann and E. L. Hahn, *Phys. Rev.* **128**, 2042-2053 (1962).

18. M. J. Duer, *Introduction to Solid-State NMR Spectroscopy*, 2004, Blackwell Publishing Ltd., Oxford.

19. D. C. Apperley, R. K. Harris and P. Hodgkinson, *Solid State NMR: Basic Principles & Practice*, 2012, Momentum Press LLC, New York.

20. G. Albrecht and R. B. Corey, *J. Am. Chem. Soc.* **61**, 1087-1103 (1939).

21. Y. Iitaka, *Acta Cryst.* **13**, 35-45 (1960).

22. Y. Iitaka, *Acta Cryst.* **14**, 1-10 (1961).

23. P.-G. Jönsson and Å. Kvick, *Acta Cryst. B* **28**, 1827-1833 (1972).

24. Å. Kvick, W. M. Canning, T. F. Koetzle and G. J. B. Williams, *Acta Cryst. B* **36**, 115-120 (1980).

25. T. N. Drebushchak, E. V. Boldyreva and E. S. Shutova, *Acta Cryst. E* **58**, o634-o636 (2002).

26. V. A. Drebushchak, E. V. Boldyreva, T. N. Drebushchak and E. S. Shutova, *J. Cryst. Growth* **241**, 266-268 (2002).

27. B. A. Garetz, J. Matic and A. S. Myerson, *Phys. Rev. Lett.* **89**, 175501 (2002).

28. E. V. Boldyreva, V. A. Drebushchak, T. N. Drebushchak, I. E. Paukov, Y. A. Kovalevskaya and E. S. Shutova, *J. Therm. Anal. Calorim.* **73**, 409-418 (2003).

29. E. S. Ferrari, R. J. Davey, W. I. Cross, A. L. Gillon and C. S. Towler, *Cryst. Growth Des.* **3**, 53-60 (2002).

30. R. E. Taylor, *Concepts Magn. Reson.* **22A**, 79-89 (2004).

31. C. S. Towler, R. J. Davey, R. W. Lancaster and C. J. Price, *J. Am. Chem. Soc.* **126**, 13347-13353 (2004).

32. I. Weissbuch, V. Y. Torbeev, L. Leiserowitz and M. Lahav, *Angew. Chem. Int. Ed.* **44**, 3226-3229 (2005).

33. M. Xu and K. D. M. Harris, *J. Phys. Chem. B* **111**, 8705-8707 (2007).

34. C. E. Hughes, S. Hamad, K. D. M. Harris, C. R. A. Catlow and P. C. Griffiths, *Farad. Discuss.* **136**, 71-89 (2007).

35. S. K. Poornachary, P. S. Chow and R. B. H. Tan, *Cryst. Growth Des.* **8**, 179-185 (2007).

36. C. E. Hughes and K. D. M. Harris, *New J. Chem.* **33**, 713-716 (2009).

37. C. Chen, O. Cook, C. E. Nicholson and S. J. Cooper, *Cryst. Growth Des.* **11**, 2228-2237 (2011).

38. G. J. Han, S. Thirunahari, P. S. Chow and R. B. H. Tan, *CrystEngComm* **15**, 1218-1224 (2013).

39. G. L. Perlovich, L. K. Hansen and A. Bauer-Brandl, *J. Therm. Anal. Calorim.* **66**, 699-715 (2001).

40. A. Théorêt, *Spectrochim. Acta A* **27**, 11-18 (1971).

41. P. A. Williams, C. E. Hughes, G. K. Lim, B. M. Kariuki and K. D. M. Harris, *Cryst. Growth Des.* **12**, 3104-3113 (2012).

42. C. E. Hughes, P. A. Williams, T. R. Peskett and K. D. M. Harris, *J. Phys. Chem. Lett.* **3**, 3176-3181 (2012).

43. J. Martí-Rujas, B. M. Kariuki, C. E. Hughes, A. Morte-Ródenas, F. Guo, Z. Glavcheva-Laleva, K. Taştemür, L.-L. Ooi, L. Yeo and K. D. M. Harris, *New J. Chem.* **35**, 1515-1521 (2011).

44. K. D. M. Harris, *J. Solid State Chem.* **106**, 83-98 (1993).

45. K. D. M. Harris, *J. Mol. Struct.* **374**, 241-250 (1996).

46. K. D. M. Harris, *Chem. Soc. Rev.* **26**, 279-289 (1997).

47. F. Guillaume, *J. Chim. Phys. (Paris)* **96**, 1295-1315 (1999).

48. M. D. Hollingsworth, *Science* **295**, 2410-2413 (2002).

49. K. D. M. Harris, *Supramol. Chem,* **19**, 47-53 (2007).

50. K. D. M. Harris, P. E. Jupp and S.-O. Lee, *J. Chem. Phys.* **111**, 9784-9790 (1999).

51. C. E. Hughes, P. A. Williams and K. D. M. Harris, in preparation.

52. D. Albesa-Jové, B. M. Kariuki, S. J. Kitchin, L. Grice, E. Y. Cheung and K. D. M. Harris, *ChemPhysChem* **5**, 414-418 (2004).

53. Owing to the proximity of the ^{1}H and ^{19}F Larmor frequencies, hardware modifications are required to convert between ^{1}H and ^{19}F NMR measurements, so it is not feasible to record both ^{1}H and ^{19}F NMR spectra in the same crystallization experiment. As a consequence, ^{1}H and ^{19}F NMR spectra were measured for two separate crystallization experiments on the same sample.

54. I. Weissbuch, F. Frolow, L. Addadi, M. Lahav and L. Leiserowitz, *J. Am. Chem. Soc.* **112**, 7718-7724 (1990).

55. F. S. Ihlefeldt, F. B. Pettersen, A. von Bonin, M. Zawadzka and C. H. Görbitz, *Angew. Chem. Int. Ed.* in press (2014).

56. M. D. King, T. N. Blanton and T. M. Korter, *Phys. Chem. Chem. Phys.* **14**, 1113-1116 (2012).

57. P. A. Williams, C. E. Hughes, A. B. M. Buanz, S. Gaisford and K. D. M. Harris, *J. Phys. Chem. C* **117**, 12136-12145 (2013).

58. E. Mossou, S. C. M. Teixeira, E. P. Mitchell, S. A. Mason, L. Adler-Abramovich, E. Gazite and V. T. Forsyth, *Acta Cryst. C* **70**, 326-331 (2014).

59. M. H. Frey, J. A. Di Verdi and S. J. Opella, *J. Am. Chem. Soc.* **107**, 7311-7315 (1985).

60. S. J. Clark, M. D. Segall, C. J. Pickard, P. J. Hasnip, M. J. Probert, K. Refson and M. C. Payne, *Z. Kristallogr.* **220**, 567-570 (2005).

61. A. L. Webber, L. Emsley, R. M. Claramunt and S. P. Brown, *J. Phys. Chem. A* **114**, 10435-10442 (2010).

62. R. K. Harris, P. Hodgkinson, C. J. Pickard, J. R. Yates and V. Zorin, *Magn. Reson. Chem.* **45**, S174−S186 (2007).

63. P. Debye, *Polar Molecules*, 1929, The Chemical Catalog Company, New York.

64. A. Nowacka, P. C. Mohr, J. Norrman, R. W. Martin and D. Topgaard, *Langmuir* **26**, 16848-16856 (2010).

65. E. V. Boldyreva, S. N. Ivashevskaya, H. Sowa, H. Ahsbahs and H.-P. Weber, *Dokl. Phys. Chem.* **396**, 111-114 (2004).

66. A. Dawson, D. R. Allan, S. A. Belmonte, S. J. Clark, W. I. F. David, P. A. McGregor, S. Parsons, C. R. Pulham and L. Sawyer, *Cryst. Growth Des.* **5**, 1415-1427 (2005).

67. E. V. Boldyreva, S. N. Ivashevskaya, H. Sowa, H. Ahsbahs and H.-P. Weber, *Z. Kristallogr.* **220**, 50-57 (2005).

68. S. V. Goryainov, E. N. Kolesnik and E. V. Boldyreva, *Physica B* **357**, 340-347 (2005).

69. S. V. Goryainov, E. V. Boldyreva and E. N. Kolesnik, *Chem. Phys. Lett.* **419**, 496-500 (2006).

70. M. Xu and K. D. M. Harris, *J. Am. Chem. Soc.* **127**, 10832-10833 (2005).

71. A. Bielecki and D. P. Burum, *J. Magn. Reson. A* **116**, 215-220 (1995).

72. A. L. Van Geet, *Anal. Chem.* **40**, 2227-2229 (1968).

73. A. L. Van Geet, *Anal. Chem.* **42**, 679-680 (1970).

74. A. E. Aliev and K. D. M. Harris, *Magn. Reson. Chem.* **32**, 366-369 (1994).

75. F. Bloch, *Phys. Rev.* **70**, 460-474 (1946).

Figures

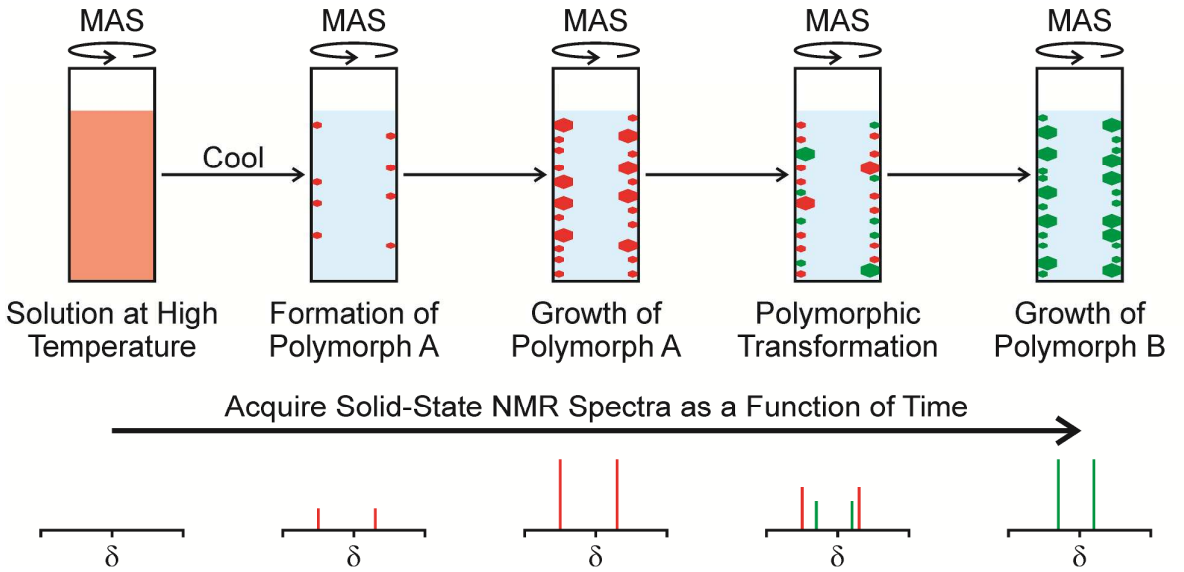

Figure 1. Schematic of the strategy for *in-situ* solid-state NMR studies of crystallization processes, illustrated by the case of a system in which the crystallization process initially produces a meta-stable polymorph A (red) followed by a polymorphic transformation to produce a more stable polymorph B (green). The corresponding changes in the measured solid-state NMR spectrum as a function of time are shown at the bottom.

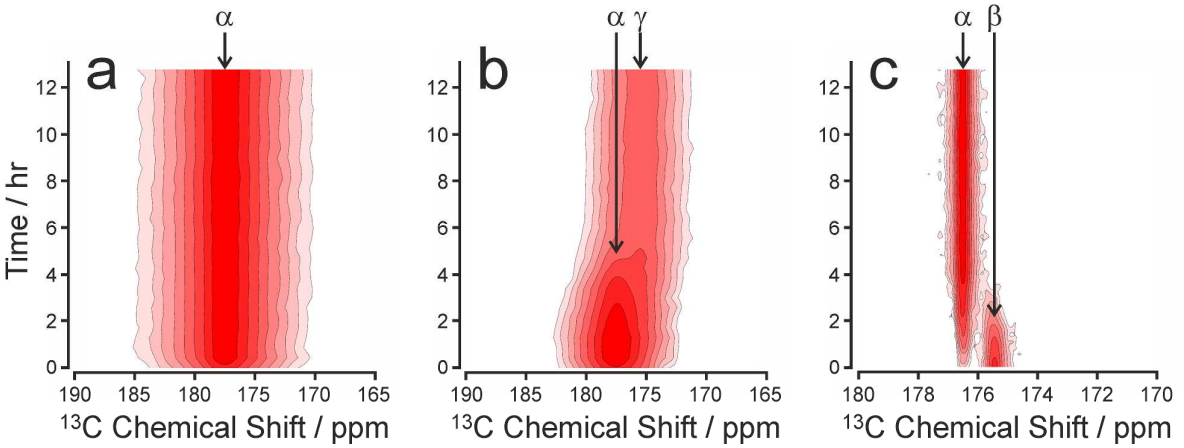

Figure 2. *In-situ* $^{1}H \rightarrow ^{13}C$ CP NMR spectra (showing only the carboxylate region) recorded as a function of time for glycine crystallizing from (a) H_2O, (b) D_2O and (c) H_2O/methanol. The known peak positions for the α, β and γ polymorphs are indicated. Note that the sample of glycine used for the experiments in (a) and (b) was ^{13}C labelled in both carbon sites, whereas the sample of glycine used for the experiment in (c) was ^{13}C labelled only in the carboxylate site. As a consequence, the ^{13}C linewidth is significantly narrower in (c). In each case, intensity contour intervals are defined on a logarithmic scale.

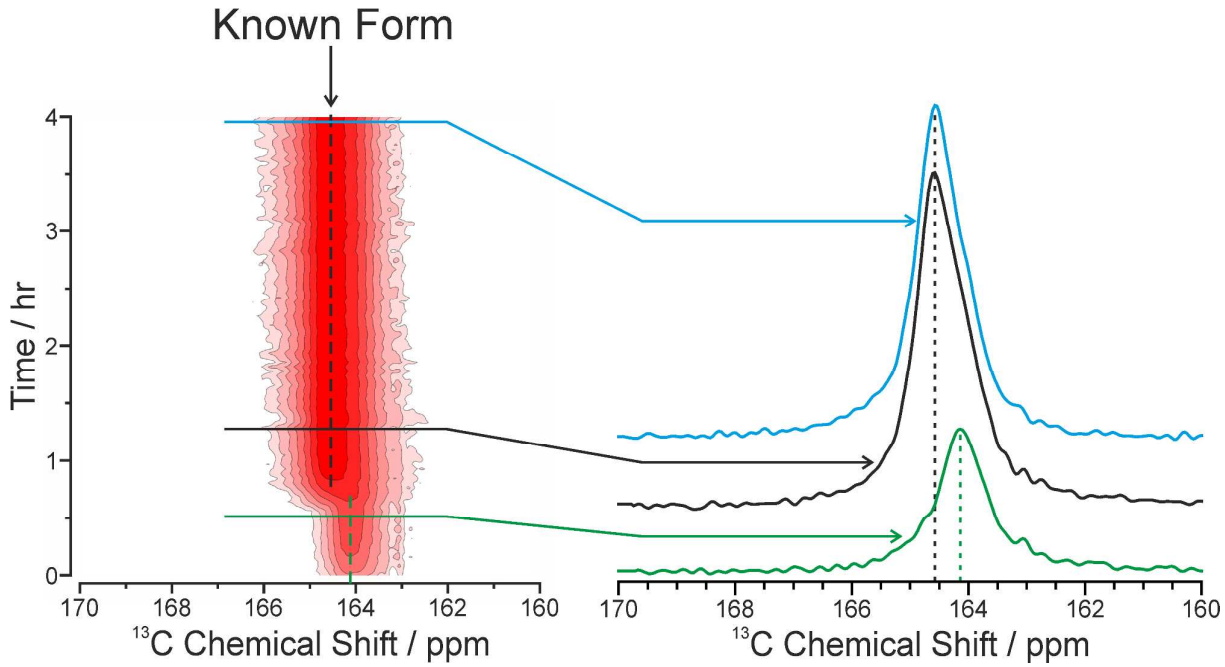

Figure 3. *In-situ* solid-state ^{13}C NMR spectra (showing the region of the spectrum containing the isotropic peak for urea) recorded as a function of time during crystallization of 1,10-dihydroxydecane and ^{13}C-labelled urea from methanol. Intensity contour intervals are defined on a logarithmic scale.

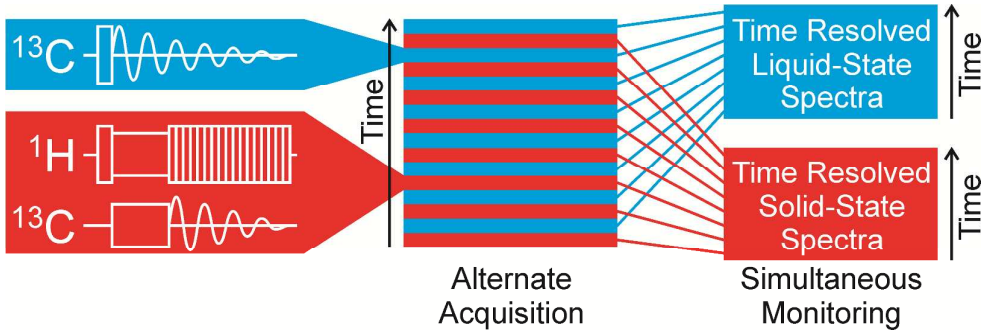

Figure 4. Schematic of the experimental procedure for CLASSIC NMR, which allows the evolution of both the solid phase and the liquid phase in a crystallization experiment to be investigated separately and simultaneously.

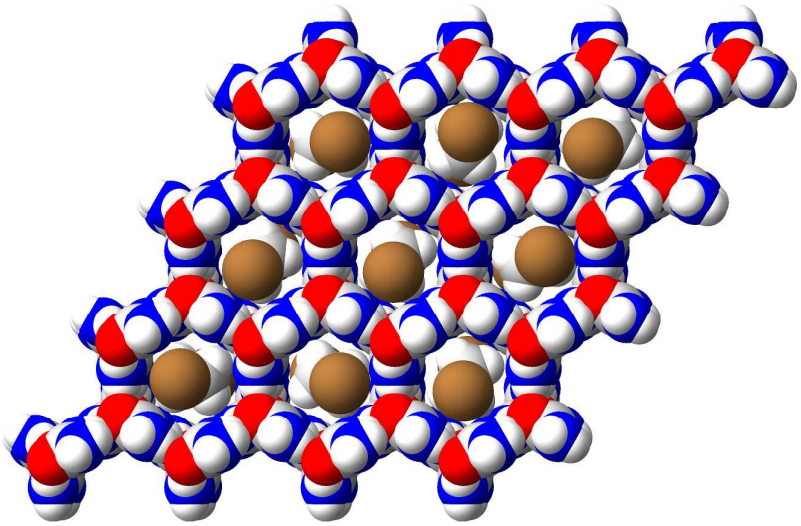

Figure 5. Crystal structure of a conventional urea inclusion compound, viewed along direction of the one-dimensional tunnels in the urea host structure.

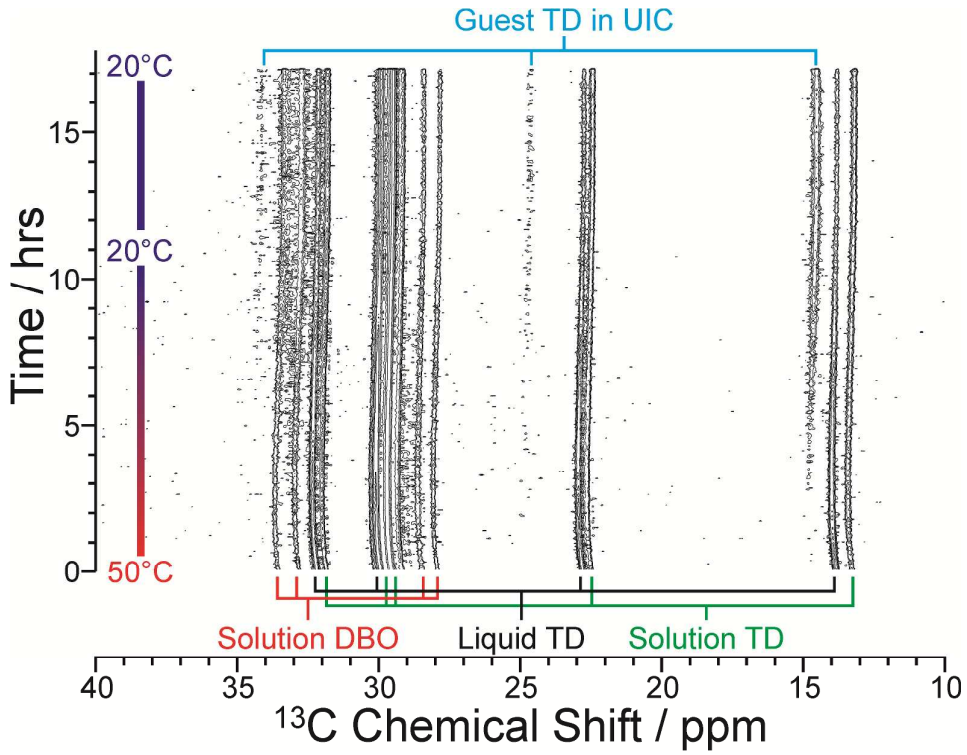

Figure 6. *In-situ* ^{13}C NMR spectra recorded using the direct-excitation ^{13}C pulse sequence during crystallization of a urea inclusion compound from a solution containing urea, 1,8-dibromooctane (DBO) and tetradecane (TD) in methanol. Peaks for the DBO and TD molecules in different phases are labelled. In addition to the solution phase and the solid (urea inclusion compound) phase, a pure liquid tetradecane phase is also present. From these results, there is no evidence for uptake of DBO guest molecules in the urea inclusion compound in this experiment.

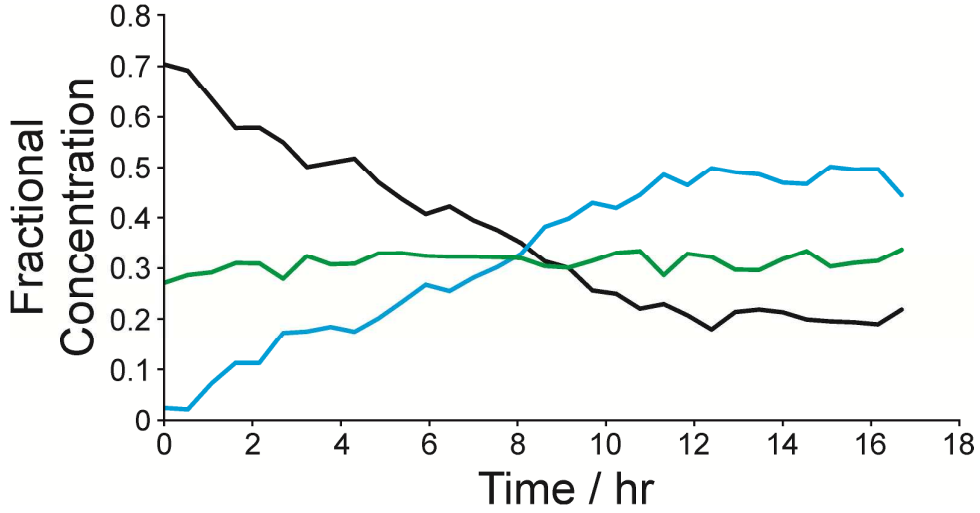

Figure 7. Time-dependence of the relative amounts of tetradecane molecules in the three distinct phases present in the crystallization system (guest molecules in the urea inclusion compound, blue; solution phase, green; pure liquid tetradecane, black) determined from the intensities of the methyl peaks in the *in-situ* ^{13}C NMR spectra.

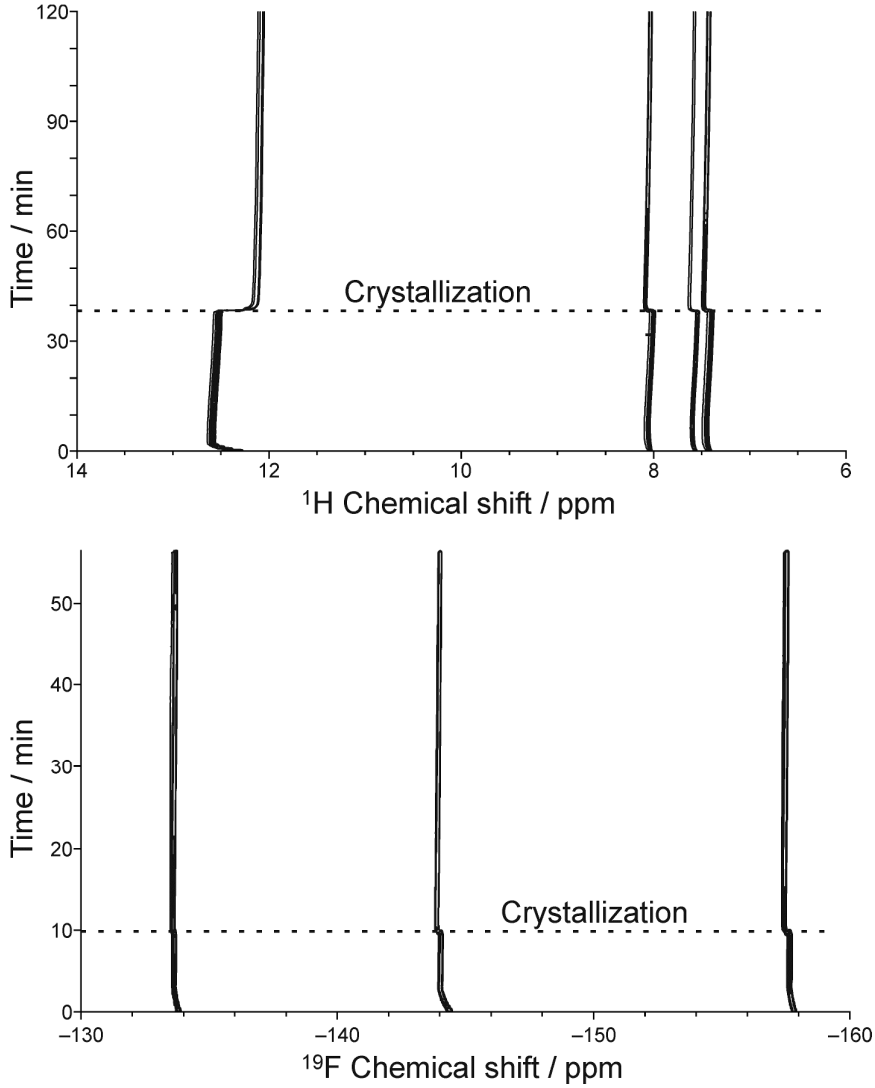

Figure 8. *In-situ* liquid-state ^{1}H NMR (top) and ^{19}F NMR (bottom) spectra recorded (in separate experiments) as a function of time for co-crystallization of benzoic acid and pentafluorobenzoic acid from d_2-dichloromethane.

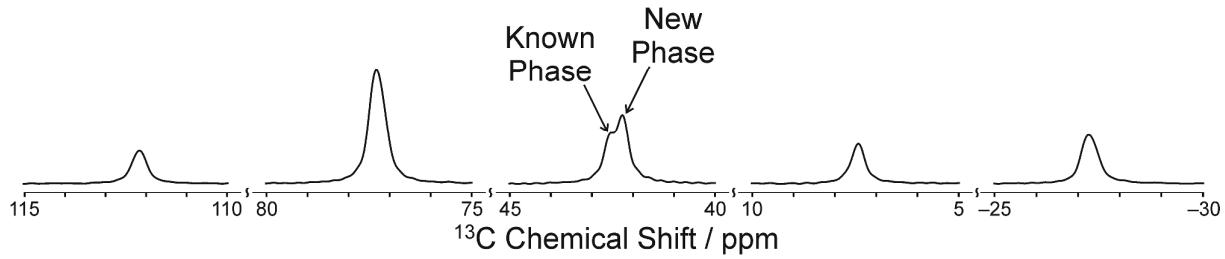

Figure 9. The first ^{1}H→^{31}P CP NMR spectrum recorded during the *in-situ* ^{31}P NMR study of crystallization of TMPO from toluene, showing the isotropic peaks (in the range 42 to 43 ppm) and several spinning sidebands.

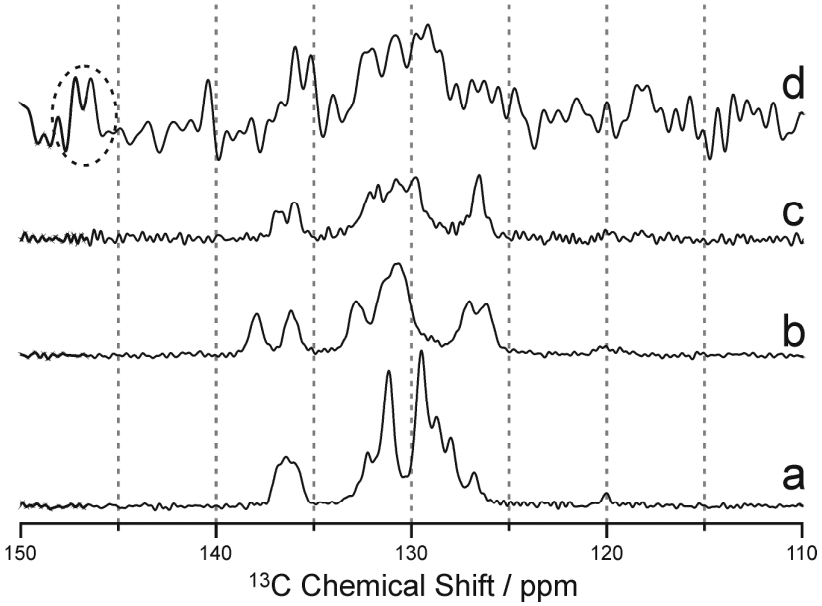

Figure 10. High-resolution solid-state ^{13}C NMR spectra (recorded using ^{1}H→^{13}C CP) for: (a) polymorph I of anhydrous L-Phe, (b) the hemihydrate of L-Phe, (c) the monohydrate of L-Phe, and (d) the solid-phase formed in our *in-situ* solid-state ^{13}C NMR study of the crystallization of L-Phe from ethanol/water (the peaks around 147 ppm discussed in the text are highlighted).

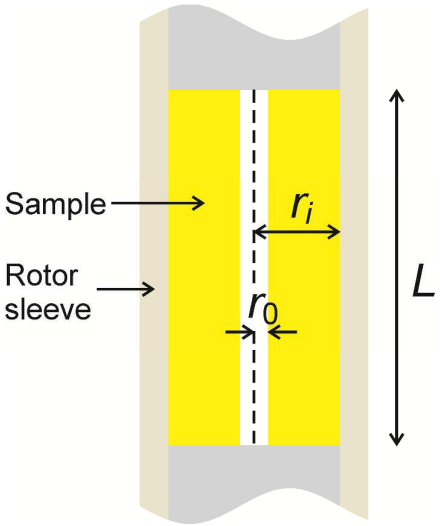

Figure 11. Schematic of a sample inside an NMR rotor undergoing magic-angle spinning, including definitions of terms used in Eqs. 2-5.

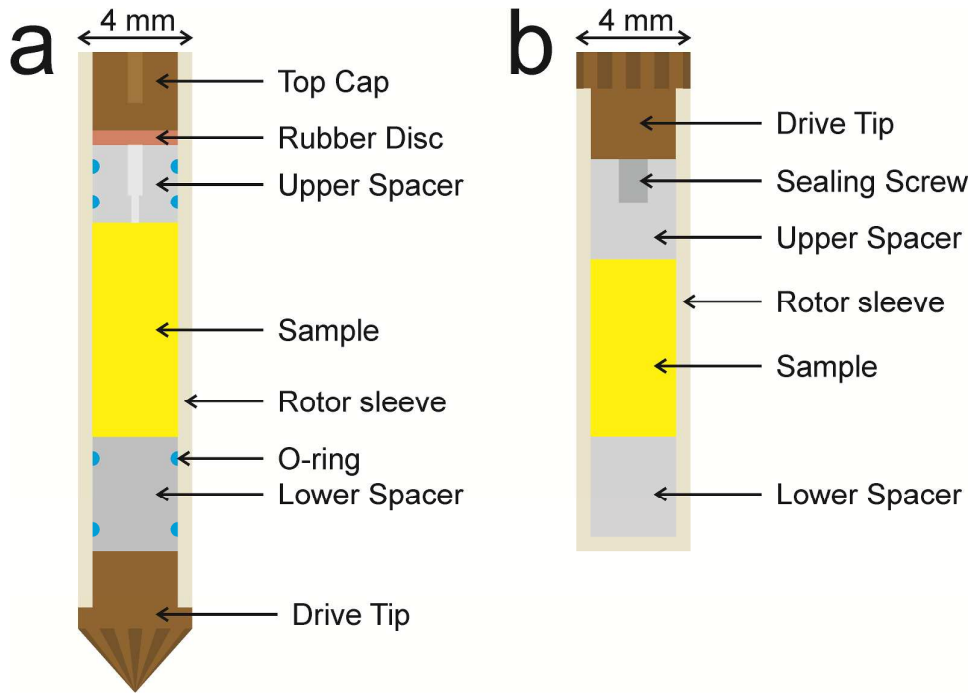

Figure 12. Examples of designs that have overcome the challenges of sealing liquid-containing samples inside NMR rotors for use in rapid MAS experiments, as required for *in-situ* solid-state NMR studies of crystallization from solution. The rotor designs shown represent schematics of sealing systems used by Varian (left) and Bruker (right).